Study The Electroosmosis Flow In Microchannel With Contractions Of Different Geometries: Part Ll

Mushtaq Ismael Hasan*, Alaa M. Lafta
Mechanical Engineering Department, College of Engineering, Thi-Qar University

Abstract:

Electrokinetic micropumps received extra attention due to its applications in pumping of biological and chemical fluids, such as blood, DNA, and saline PBSs. In this paper the electroosmotic flow in microchannel has been numerically investigated by developing a model from the basic governing equations (continuity, momentum, energy, and Laplace and Poison-Boltzmann equations) through a square channel with contraction of different geometries. Utilizing the numerical analysis, a mathematical model has been built in order to study the electroosmosis-based microflow of the negatively charged messenger proteins to the negatively charged nucleus to shed more light on the electroosmotic flow behavior through microchannels with contraction. The results obtained show a considerable effect of the zeta potential on the velocity and many parameters studied such as shapes, depth and number of contractions and channel wall material. Adding materials with different thermal conductivity to channel wall, affect the heat distribution throughout channel length. In particular, five wall materials typically used in Microelectromechanical systems (MEMS). It shows that a material with low thermal conductivity works as isolation against dissipating the heat generated from Joule heating effect.

Keywords: electroosmotic flow; microchannel; micropump; numerical investigation; electrokinetic flow; contraction,

دراسة الجريان التناضحي بالقنوات الدقيقة مع اشكال مختلفة من التخصرات: الجزء II

الخلاصه:

تستقطب المضخات الكهروحركية الكثير من الاهتمام وذلك لتطبيقاتها بضخ السوائل الكيمائية والبايلوجية مثل الدم وبصمه الدم الوراثية والسائل الحيوي(PBS) .في هذة الورقة البحثية يتم دراسة ظاهرة التناضح الكهربائي في القنوات الدقيقة عدديا بواسطة بناء نموذج رياضي من المعادلات الحاكمه (معادلة الاستمراريه والحركية والطاقة والكهربائيه) خلال قناة مربعه المقطع العرضي. لتسليط الضوء على سلوك الجريان التناضخي في القنوات الدقيقة سيتم دراسة هذة القنوات مع تخصر. تبين النتائج المستحصلة من حل النموذج تاثير تغير قيمه السرعه نتيجه لتغير قيمه الفولطيه الداخلية المتواجدة على الجدار (ζ) وكذلك دراسة تاثير عدة عوامل وهي عمق وعدد وشكل التخصر في القناة الدقيقه بالاضافة الى دراسه تاثير تغيرنوع المادة العازله الكهربائية لجدار القناه المدروسة. حيث وجد ان لتغير نوع العازل المستخدم وبالتالي يتغير مقدار الموصلية الحرارية بالصورة المباشره و ان لهذا التغير تاثير مباشر على توزيع درجة الحراة ومقدار التبدد الحراري ومن المهم فهم ضروره التخلص من الحرارة المتولد عن طريق الحرارة المتولدة (Q) بالاجهزه المايكرويه لما فيها من ضرر على هذة الاجهزه

List of symbols:

symbol	***Description***	***unit***
u_{EO}	Velocity electroosmosis	m/s
μ_{EO}	mobility electroosmosis	$m.(s.V)^{-1}$
ε	*Permittivity*	$\boldsymbol{Cm^{-1}\ V^{-1}}$
ζ	*zeta potential*	$\boldsymbol{Vm^{-1}}$
μ	*Viscosity*	$\boldsymbol{Nsm^{-2}}$
E	*external electric field*	$\boldsymbol{V}$
ρ_e	*surface charge density*	$\boldsymbol{Cm^{-3}}$
Q	*joule heating*	$W\ m^{-3}$

1. Introduction:

Generally electro kinetics is the combination of "electric" plus "kinetics", in other word the electrokinetics is the motion of liquid or particle under the influence of electric field. Electrokinetics categorized to, electro-osmosis, which is the motion of a liquid with respect to a solid surface through the application of an external electric field, electro-phoresis which is the motion of charged particles with respect to a solid surface with the application of an external electric field, streaming potential which is generated by applied electric field by ionised liquid flowing past a solid surface (opposite of electro-osmosis) and sedimentation potential which is the generating of an electric field by charged particles moving with respect to a stationary solid wall surface (opposite of electrophoresis). Electroosmosis is caused by the presence of the electrical double layer, formed at the fluid/solid or fluid/membrane interface, and by the action of the electric field parallel to this interface. The flow of the fluid results in the movement of the particles immersed in the fluid. Many researchers using different research methodologies and various analytic methods have studies the parameters that might affect electrokinetically-driven flow. The majority of these studies have employed Debye-Huckel linearization to simplify the sophisticated theoretical computations. Moreover, to make use of Newton's law of viscosity researchers often consider Newtonian fluids. Following are selected examples of these studies. Recently, an analytical solution for electroosmotic flow in a cylindrical capillary was derived by Kang et al. [1]. They solved the complete Poisson–Boltzmann equation for arbitrary zeta-potentials. Wang et al. [2] examined the hydrodynamic aspects of fully developed electroosmotic flow in a semicircular microchannel. In contrast, Xuan and Li [3] developed general solutions for electrokinetic flow in microchannels with arbitrary geometry and arbitrary distribution of wall charge. Electroosmotic flow in parallel plate microchannels for the cases in which electric double layers interact with each other was analyzed by Talapatra and Chakraborty [4]. Hydro dynamically developing flow between two parallel plates for electroosmotically generated flow has been numerically analyzed by Yang et al. [5]. Maynes and Webb [6] analytically studied fully developed electroosmotically generated convective transport for a parallel plate microchannel and circular microtube under imposed constant wall heat flux and constant wall temperature boundary conditions. Yang et al. [7] investigated forced convection in rectangular ducts with electrokinetic effects for both hydrodynamically and

thermally fully developed flow. Chang‐Yi W. et.al (2016) [8] developed an approach to analytic solutions for electroosmotic flow in micro‐ducts by examining functions of the Helmholtz equation. G.C. Shit et.al (2016) [9] studied the electro-osmotic flow of power-law fluid and heat transfer in a micro-channel with effects of Joule heating and thermal radiation. In our previous paper M. I. Hasan and Alaa M. L. (2017) [10] shown the contours of velocity distribution for the four shapes of contractions; rectangular, triangular, trapezoidal and curved. It is seen from these figures that the triangular contraction cause higher value for velocity. The temperature distribution contours for the same four microchannels with different shapes of contractions, show that, highest temperature has been recorded in the rectangular contraction case. The electroosmosis velocity increased when the external applied electric field increased within the range (1000-100000V/m) at constant electroosmosis mobility. In this paper extra affecting geometrical parameters on the electroosmotic flow such as number and thickness of contractions will be studied.

2. Problem Description:

One of the well-known applications of electroosmotic flow is the mixing which mainly used in bio medical fluid applications for mixing some bio fluid in order to test it (as shown fig.1). The mixing the problem studied involves understanding the behavior of transporting a fluid via microchannel with different geometries of contraction as showen Figures (1) & (2). Following are the geometrical description and dimensions of the studied model:

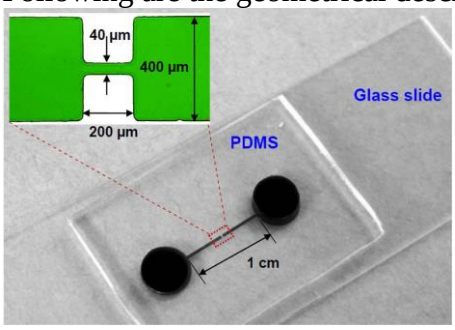

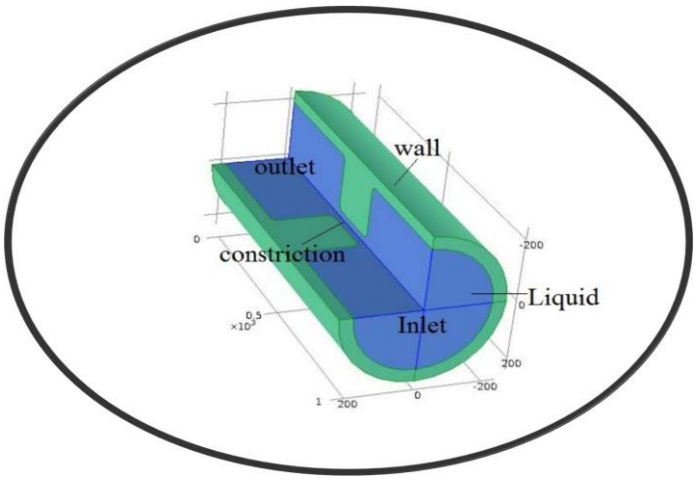

Fig (1) Typical example of problem setup (Sriram Sridharan [11]) and Fig (2) Typical schematic for studied model

- Axisymmetry
- Length 1000 µm.
- Outer radius 250 µm.
- Inner radius 200 µm.
- Contraction length 200 µm.
- Contraction radius 20 µm.

In order to study the potential effect of contraction shape on the electroosmosis flow,four microchannelshave been adopted with four different contraction shapes; namely, rectangular, traingular, trapizoidal and curved. Fig.(3) shows the geometrical details of these contraction in terms of shape and dimensions.

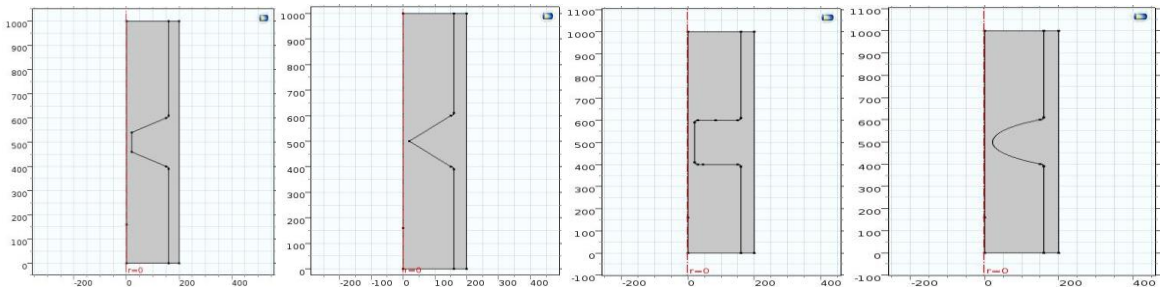

Fig(3) Shapes of contractions studied (2DAxisymmetry)

Also some new suggestions have been made in this paper in order to enhance the mixing process. In this context multiple contractions mixing section has been studied for all selected shapes of contraction as shown in fig (4).

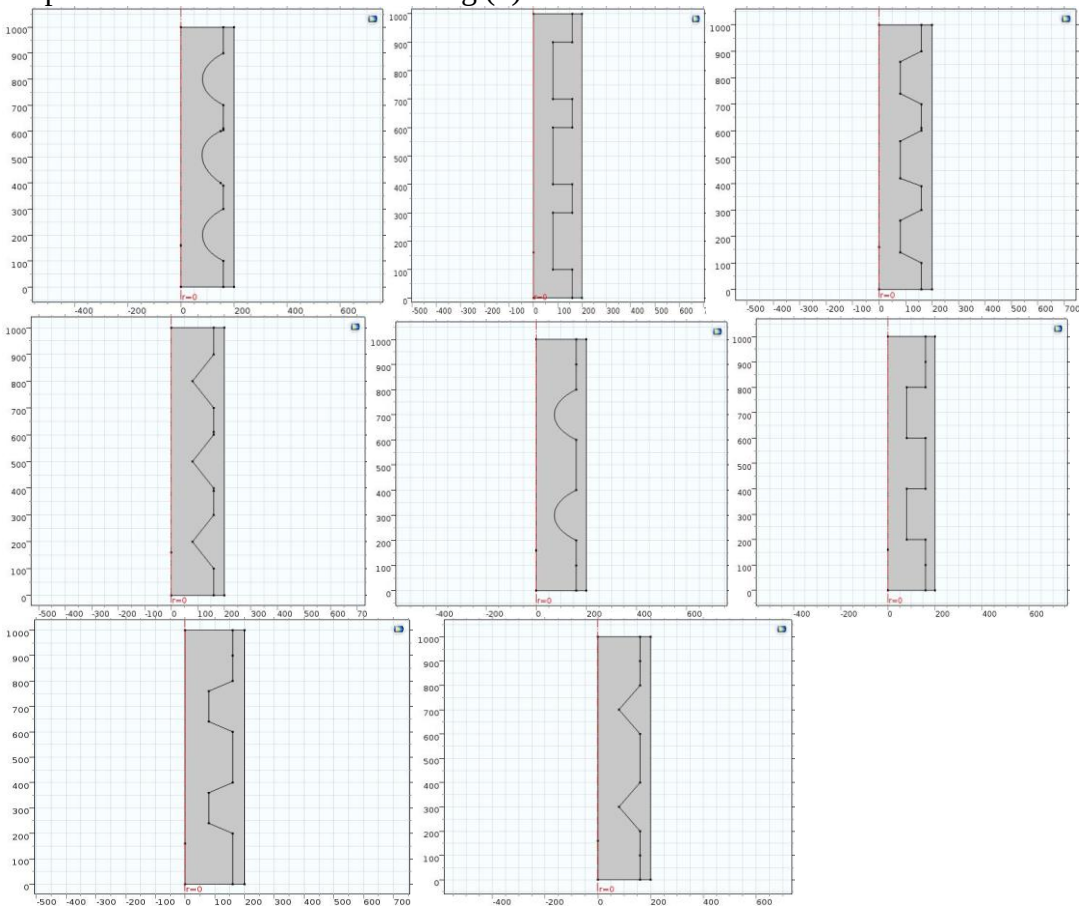

Fig. (4) different numbers of these contraction in terms of shape and dimension. (2DAxisymmetry)

3. Mathematical Formulation:

3.1. Numerical modeling:

CFD Software has been used to implement the finite element approach to solve sets of partial differential equations. Our model utilized the following predefined templates:-"physics interfaces": Electric Currents: Ac/Dc Module - Electric currents (DC) , Creeping Flow, and Heat transfer Module – Conjugate heat transfer (Laminar flow); in the stationary (in the time independent mode) [13]-[17].

Governing equation:

$$u_{EO} = \mu_{EO} E \quad (1)$$

$$\mu_{EO} = \frac{\varepsilon \zeta}{\mu} \quad (2)$$

Continuity equation:

$$\nabla^2 u = 0 \quad (3)$$

Momentum equation: $\rho \partial u/\partial t + \rho u.\nabla u = -\nabla p + \mu \nabla^2 u + \rho_e E$ (4)

possion-boltzmann equation: $\nabla^2 \phi = 0$ (5)

Energy equation: $\rho C_p \partial T/\partial t + \rho C_p u .\nabla T = \nabla .(k \nabla T) + Q$ (6)

$$Q = \nabla.(\sigma E) \quad (7)$$

Five materials have been used as a wall material for microchannel namely (PDMS, Sio_2, PMMA $Si_3 N_4$ and Polyetheline) with properties as listed in table (1)

Table 1 lists the materials included with their related properties.

Name of properties	PDMS	Sio_2	PMMA	$Si_3 N_4$	Polyetheline	Unit
Electric conductivity{σ}	0	10^{-8}	0	10^{-10}	10^{-14}	S/m
Coefficient of thermal expansion{∝}	$9*10^{-4}$	$0.5*10^{-6}$	$70*10^{-16}$	$2.3*10^{-6}$	$150*10^{-6}$	1/K
Heat capacity of constant pressure{cp}	1460	730	1420	700	1900	J/(Kg.K)
Relative permittivity {ε}	2.75	3.9	30	7.5	2.3	1
Density {ρ}	970	2200	1190	3100	930	Kg/m
Thermal condu-ctivity{K}	0.16	1.4	0.19	20	0.38	w/(m.k)

3.2 BOUNDARY CONDITION

Figure 4 below depicts the boundary conditions of both heat and flow.

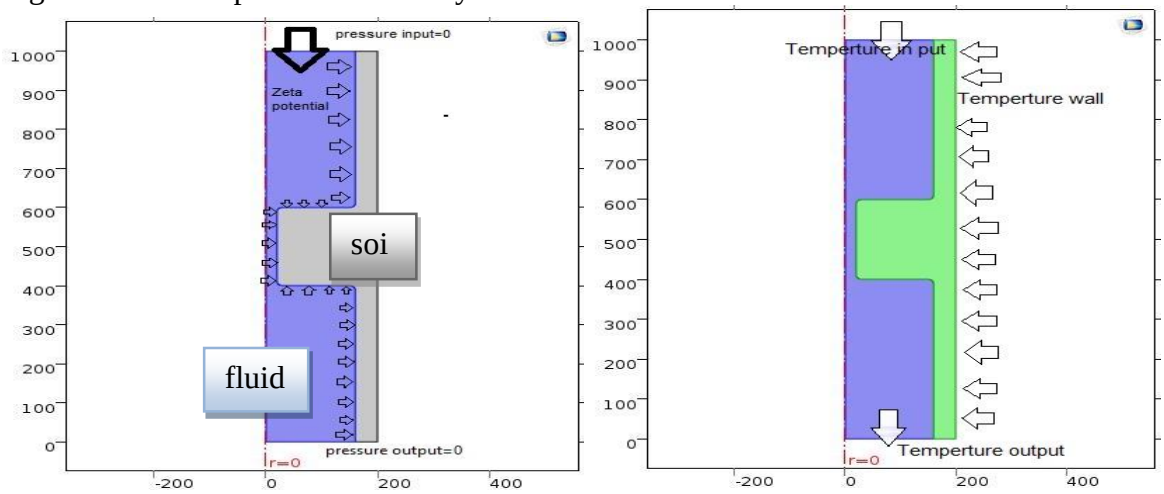

(a) fluid boundary condition (b) heat boundary condition

Fig. (4) boundary conditions used

Table (2) boundary conditions used

Location	Boundary conditions	Description
channel inlet	$T=T_{in}, u=v=w=0, P=0,$ $\emptyset = E_z L \quad , \quad \frac{\partial \Psi}{\partial z} = 0$	inflow
channel outlet	$T=T_{out}$, $P=0, \emptyset = 0, \quad \frac{\partial \Psi}{\partial Z} = 0, \frac{\partial u}{\partial z} = \frac{\partial v}{\partial z} = \frac{\partial w}{\partial z} = 0$,	fully developed
Side walls	$u=v=w=0, \Psi = \zeta,$ $\frac{\partial \emptyset}{\partial y} = 0 \quad , \quad \frac{\partial T}{\partial y} = 0, \quad \frac{\partial p}{\partial y} = 0$	No slip constant zeta potential

3.3 Mesh: *The default–physics controlled meshing was used with the option the "finest" or the second "finest" mesh selected to ensure proper conversion and precision of the calculations. Mesh in the axisymmetric model contained: 6480 triangular elements, 377*

quadrilateral elements, 434 edge elements, and 12 vertex elements. Average mesh quality of 0.94. as shown in figure 6.

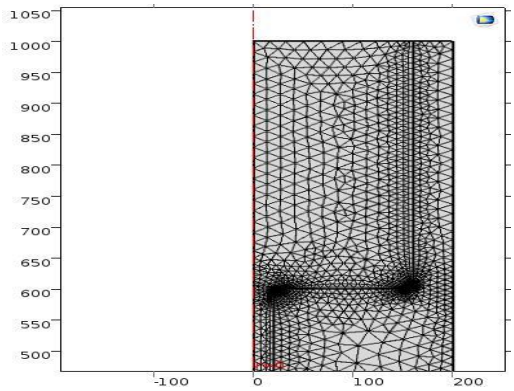

Fig. 6 Meshed model

4. Result and discussion:

4.1. Validation:

The built numerical model is used to study the mixing process in microchannel with contraction and the effect of most affecting parameters such as shape of contraction, number of contractions, and width of contraction on the mixing process in electroosmotic flow. Before using the built numerical model to analyze factors that might affect the electroosmotic micro flow characteristics, it is important as a first stage to examine the accuracy and applicability of the model developed in the current paper simulation software. In so doing, the developed model results have been compared with the analysis results obtained by sanjay [12]. Figure (7) shows the velocity profile in center line along channel length as a comparison between present model and sanjay model [12].

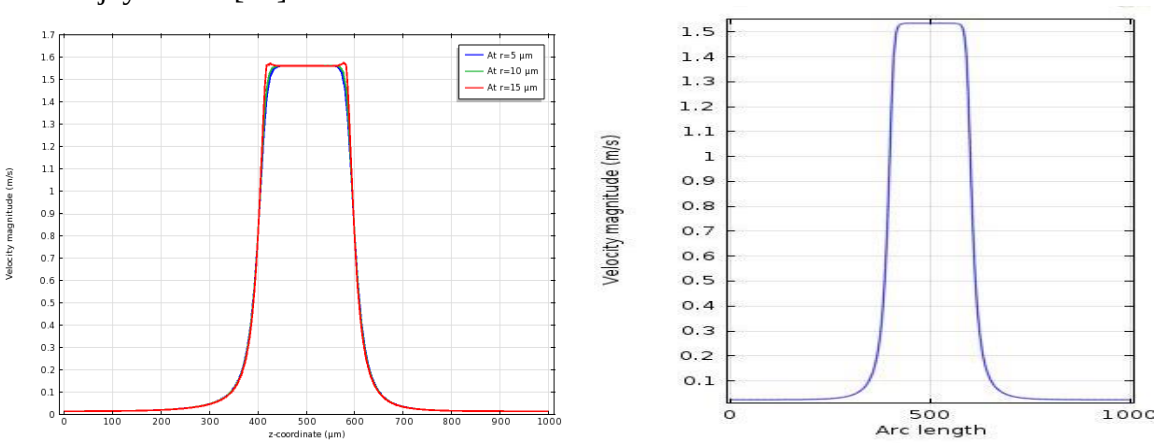

(a) sanjay's model (b) present model

Fig. 7: Velocity profile in center line along channel length as a comparison between present models and [12].

Additionally, Figure (8) depicts the velocity contours as comparison between present model and [11].

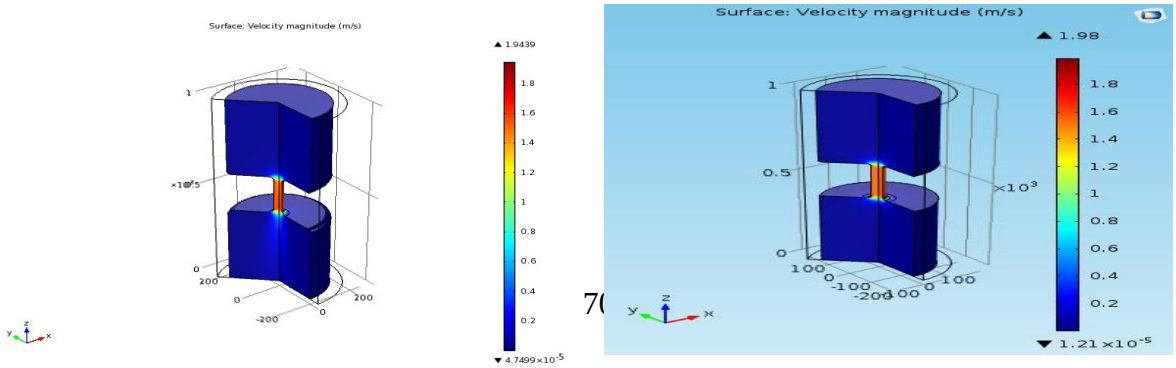

Fig. 8: Velocity contours as a comparison between present model and [12]

It is evident from Figures(7) and (8) that the present numerical model is accurate and can be safely used for further calculation due to the excellent agreement between its results and Sterm's model results; in numbers, maximum error is 2.6% and average error is 0.28%

4. 2 Effect of contraction shapes

A study of potential effect of channel contraction shape on the electroosmotic velocity is also presented. Fig. 9 (a) shows the contour plot of 40 micron depth rectangle shaped contraction. Similar effects for curvature, trapezoidal and triangular contraction shapes can be also seen in Fig. 9 (b), (c), (d) respectively. The comparison reveals that triangular shape contraction channel of 40 μm depth showed better mixing. It is useful to report that all other parameters are held constants. Such parameters are heat condition, electric voltage, fluid characteristics, wall characteristics, and channel size.

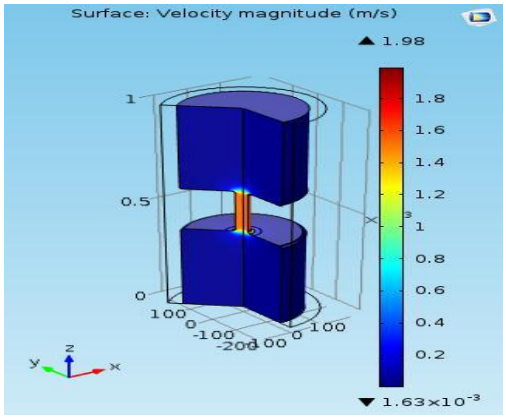

(a) rectangular contraction

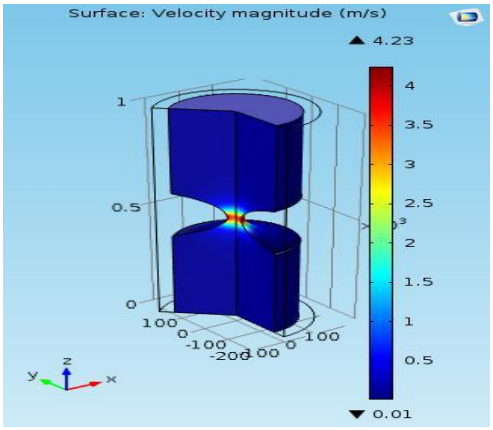

(b) curvature contraction

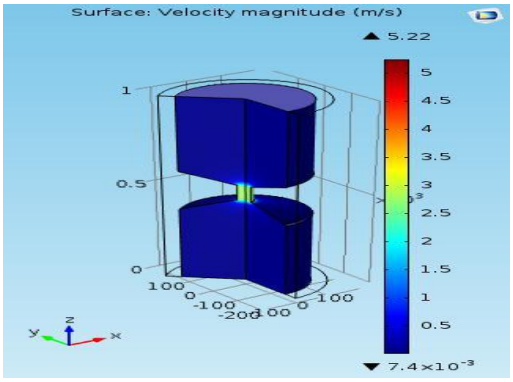

(c) trapezoidal contraction

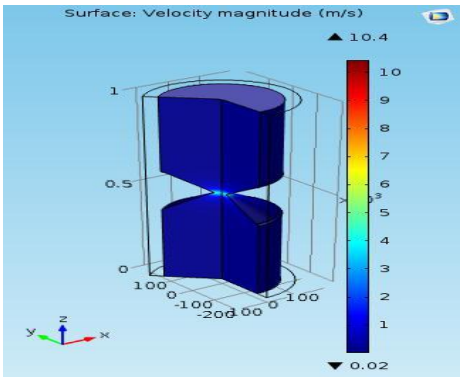

(d) triangular contraction

Fig. (9) Velocity contours distribution for different shapes of contraction at zeta potential -50 mV and $E_Z = 500000$. (a) rectangular, (b) curvature, (c) trapezoidal and (d) triangular.

Similarly, Fig.(10) is a graphical representation for the temperature distribution contours for the same four microchannels with four different shapes of contractions ((a) rectangular, (b) curvature, (c) trapezoidal and (d) triangular). Other typical boundary conditions are assumed to be constant. For obvious reasons, the presence of Joule heating will generate temperature that increase proportionally along the microchannel to reach its maximum value at the neck (contraction). Through the channel contraction flow velocity increases suddenly causing a reduction in the Joule heating effect and hence a drop in temperature generated at the contraction. On the other hand, highest temperature has been recorded in the rectangular contraction case.

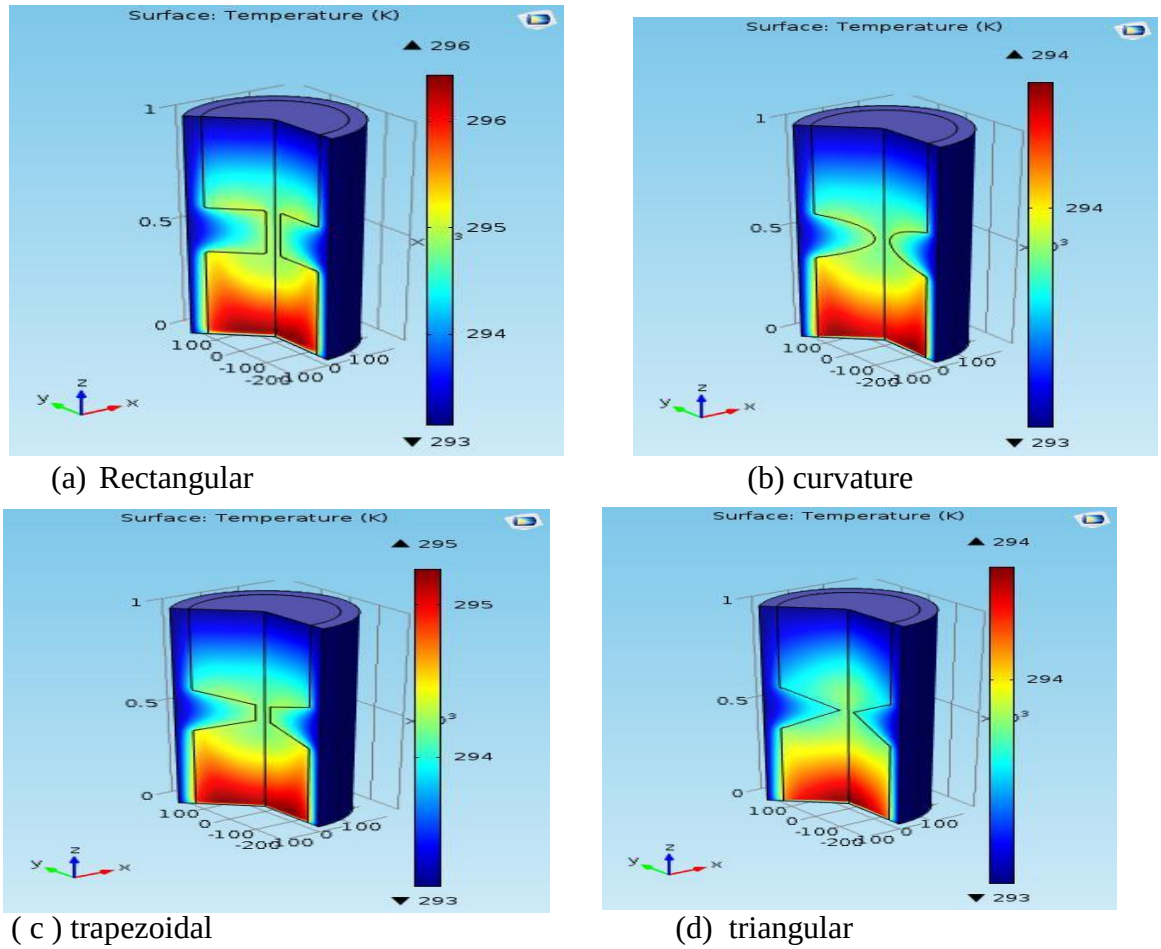

(a) Rectangular (b) curvature

(c) trapezoidal (d) triangular

Fig. (10) Temperature distribution contours for different shapes of contraction (curvature, square, trapezoidal and triangular) at zeta potential -50 mV Ez=500000.

4.3 Effects of zeta potential and wall material

In order to examine the impacts of different zeta potential values on maximum flow velocity through the four microchannels, figure (11) has been constructed. The figure reveals that the maximum velocity increases as applied zeta potential increases ($u_{eof}=E_x \mu_{eof}$) for all contraction shapes. That is obviously because the electroosmosis phenomenon is highly dependent on zeta potential.

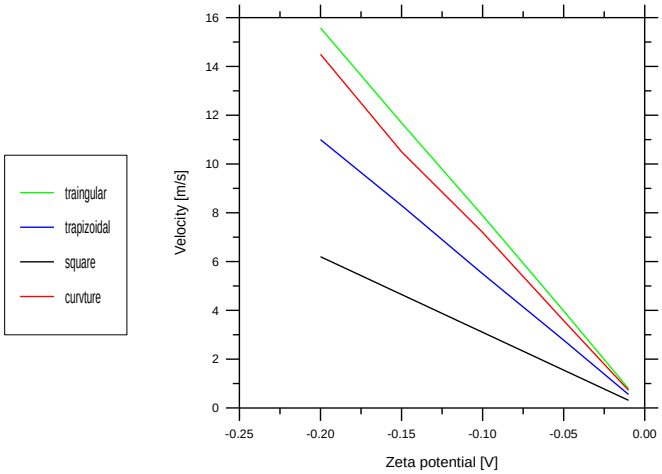

Fig. (11) Variation of maximum velocity with different values of wall zeta potential for different contraction shapes.

The analysis results also revealed that using materials with different thermal conductivity in the channel wall can affect heat distribution throughout channel length. In particular, five wall materials typically used in Microelectromechanical systems (MEMS) have been utilized Other parameters such as voltage, fluid characteristics, temperature ($T_{IN}=T_{OUT}=T_{WALL}=273$) held constant. Fig.12 shows that materials with low thermal conductivity works as isolator against dissipating the heat generated from Joule heating effect. In other words, low conductivity materials restrict heat transfer through channel wall and hence raising liquid temperature.

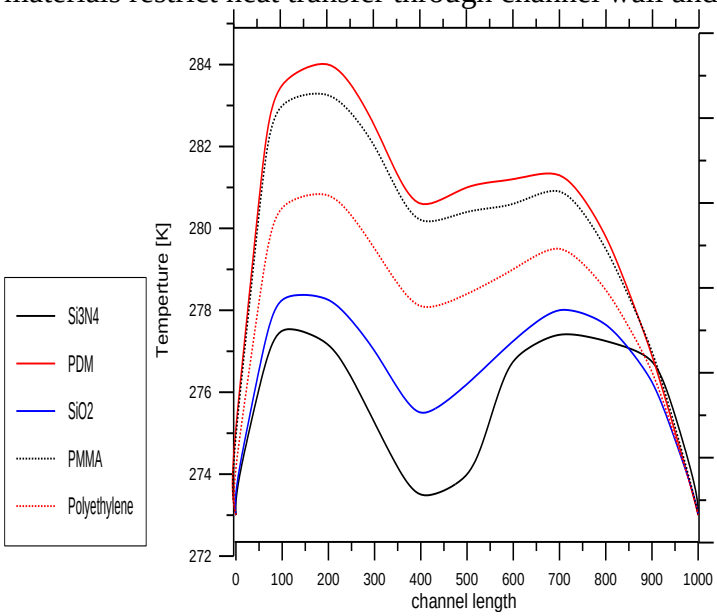

Fig. (12) Temperature distribution for different channel wall materials.

4. 4 Effect of contraction Depth

Figures 13 through 16 present three dimensional graphical illustration concerning to what extent could contraction depth affect the microflow velocity in four microchannels with rectangular, curvature, trapezoidal and triangular contraction shapes respectively. For each figure (contraction shape), the contraction distances from channel inlet is 400 mμ and applied voltage is 50 mv. Three contraction depth values have been examined; in numbers, 80, 120 and 160 mμ. In order to obtain clear understanding, these studied contraction depths can be compared with the typical contraction depth of 40 mμ shown in Figure 9.

The four figures (Figure 13 through 16) point out that, for each contraction shape, as contraction depth increases the maximum microflow velocity value decreases. This could contradict the

principles of fluid mechanics for ordinary-scale channels; that is typically an increase in channel depth would reflect a decrease in fluid flow disruption and hence an increase in flow velocity. This is, however, not true in electroosmotic fluid flow in microchannels. That is because volume-surface area ratio plays a dominant role. When contraction depth increases, then surface area will increase and hence volume-surface area ratio will go down. In other word, when width of contraction increased the effect of zeta potential will decrease because reduce the motivation of flow (ζ)

Table 2 summarizes the relationship between electroosmotic maximum velocity and contraction depth for various contraction shapes. The listed results show clearly how the increase in microchannel contraction depth could result in decreasing in the electroosmotic velocity. Analysis results reveal that mixing process can be significantly enhanced by changing microchannel geometry; in particular, contraction shape, contraction depth and contraction distance from channel inlet.

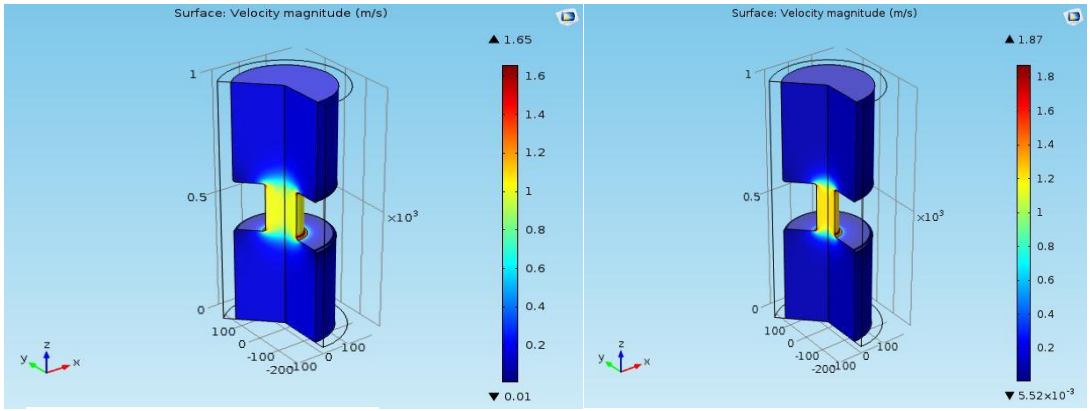

(a) depth = 80 µm (b) depth = 120 µm

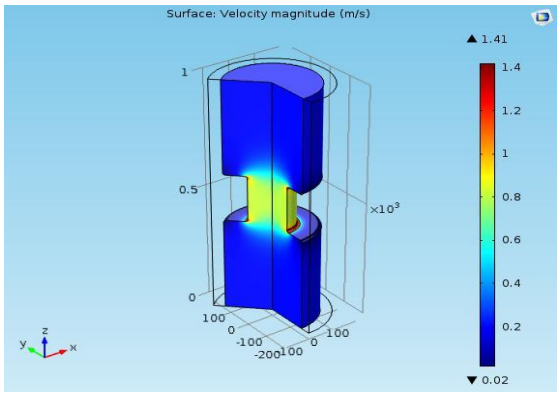

(c) depth = 160 µm

Fig.(13) Three dimensional contour for rectangular contraction with three different depths.

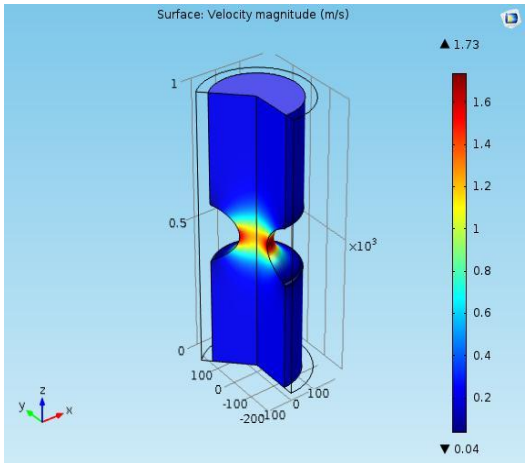

(a) depth = 80 µm

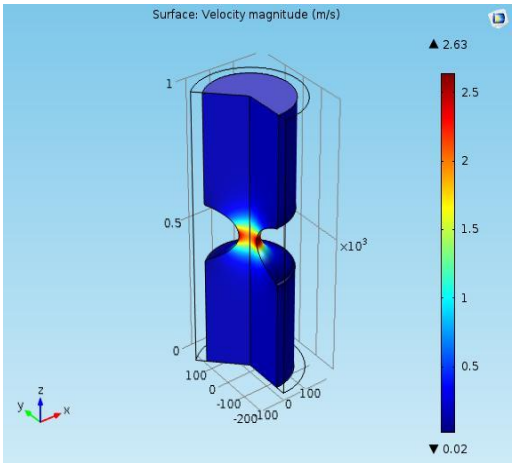

(b) depth = 120

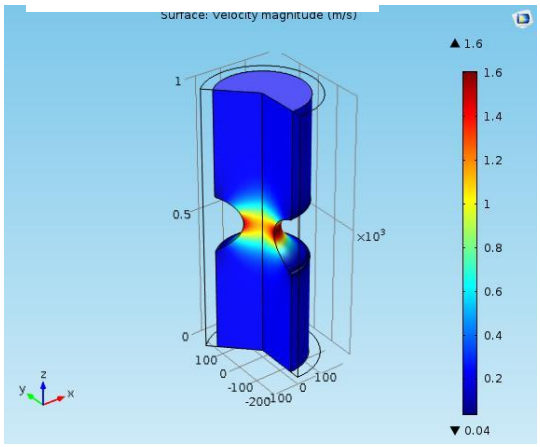

(c) depth = 160 µm

Fig. (14) Three dimension velocity contour for curvature contraction with three different depths.

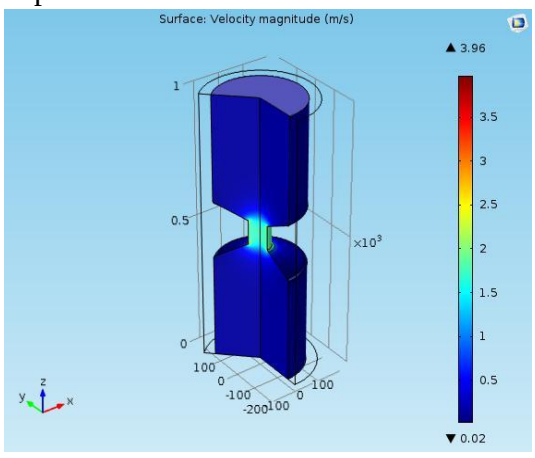

(a) depth = 80 µm

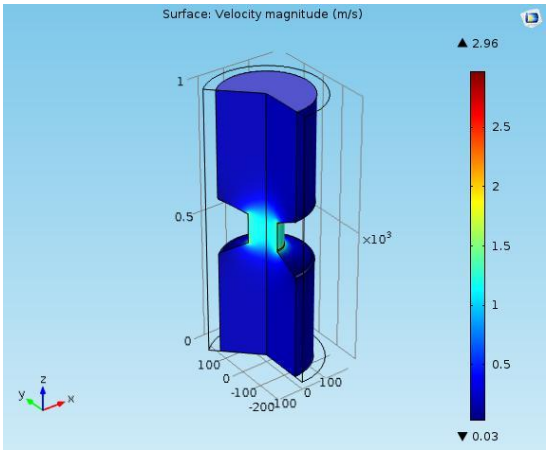

(b) depth = 120 µm

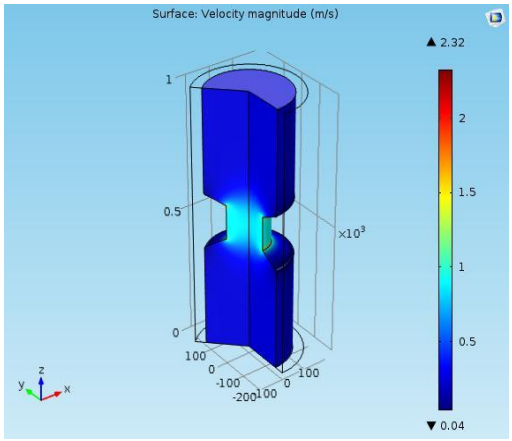

(c) depth = 160 µm

Fig. (15) Three dimensional contour for trapezoidal contraction with three different depths

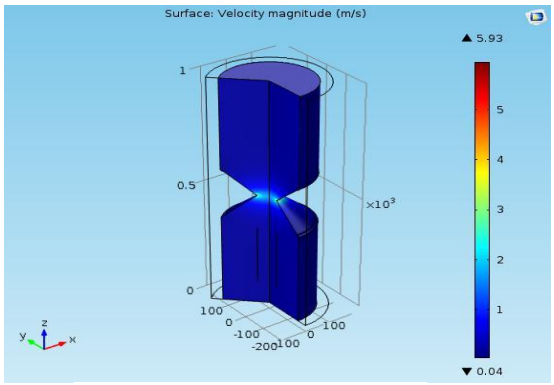

(a) depth = 80 µm

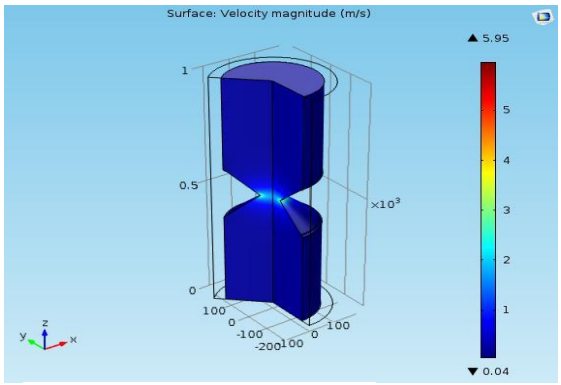

(b) depth = 120 µm

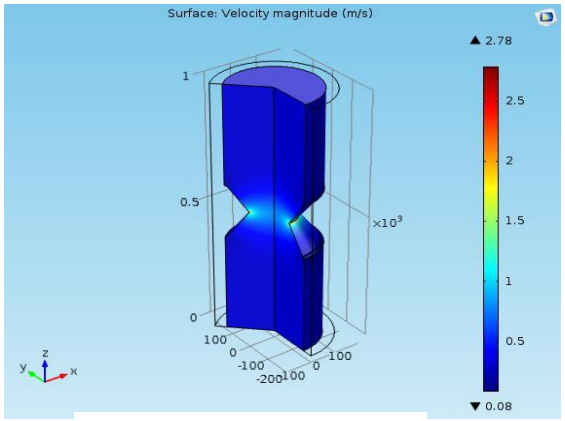

(c) depth = 160 µm

Figure (16) Three dimensional contour for triangular contraction with three different depths.

Table (3) Variation of electroosmotic maximum velocity with contraction depth (μm) for various microchannel contraction shapes.

Contraction shape	Velocity			
	Depth = 40	Depth = 80	Depth = 120	Depth = 160
Rectangular	1.98	1.87	1.65	1.41
Curvature	4.23	2.63	1.73	1.60
Trapezoidal	5.22	3.96	2.96	2.32
Triangular	10.4	5.93	5.95	2.75

4. 4 Effect of numbers of contractions

It is important to investigate the possible impacts of replacing a single contraction by a series of contractions on the electroosmosis velocity magnitude. In particular, the impacts of using microchannels with double and triple contractions for various contraction shapes have been examined. Figures 17 and Figure 18 show the velocity profile across microchannel width at the downstream position of 200μm with two contractions separated by 80μm gap for each of them. Four contraction shapes have been considered; rectangular, curvature, trapezoidal and triangular. The figures demonstrate that the mixing performance for double contraction microchannels has increased for triangular and rectangular contractions respectively. These incremental values are much higher than their corresponding values for single contraction channels. This is expected because the use of double contraction produces multiple vortices at every contraction end which is already two times the one produced using single contraction. This will obviously increase the mixing performance by enhancing the diffusion. This can be clearly noticed as a streamline plot of velocity field in a double contraction for all shaped contraction channel in Figure 18.

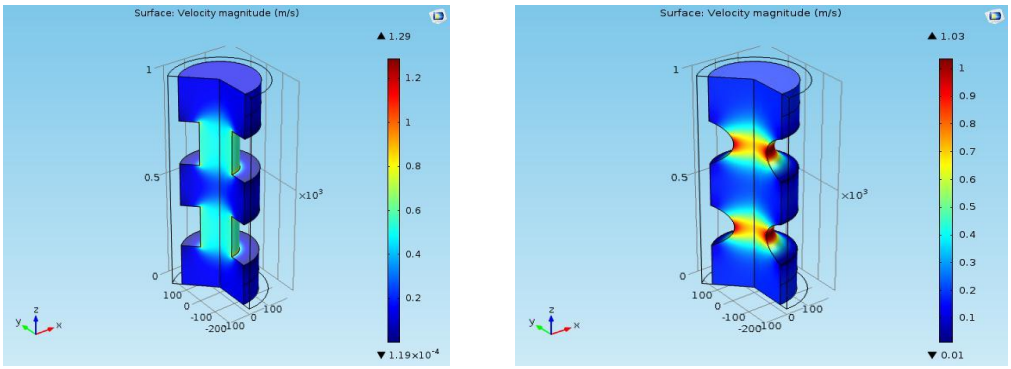

(a) Rectangular (b) Curvature

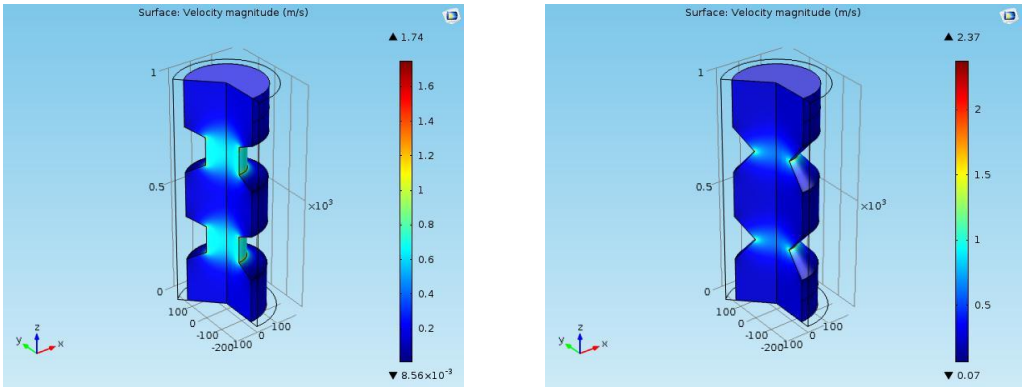

(c) Trapezoidal (d) Triangular

Figure 17: Three-dimensional contour for double contraction microchannel with different contraction shapes.

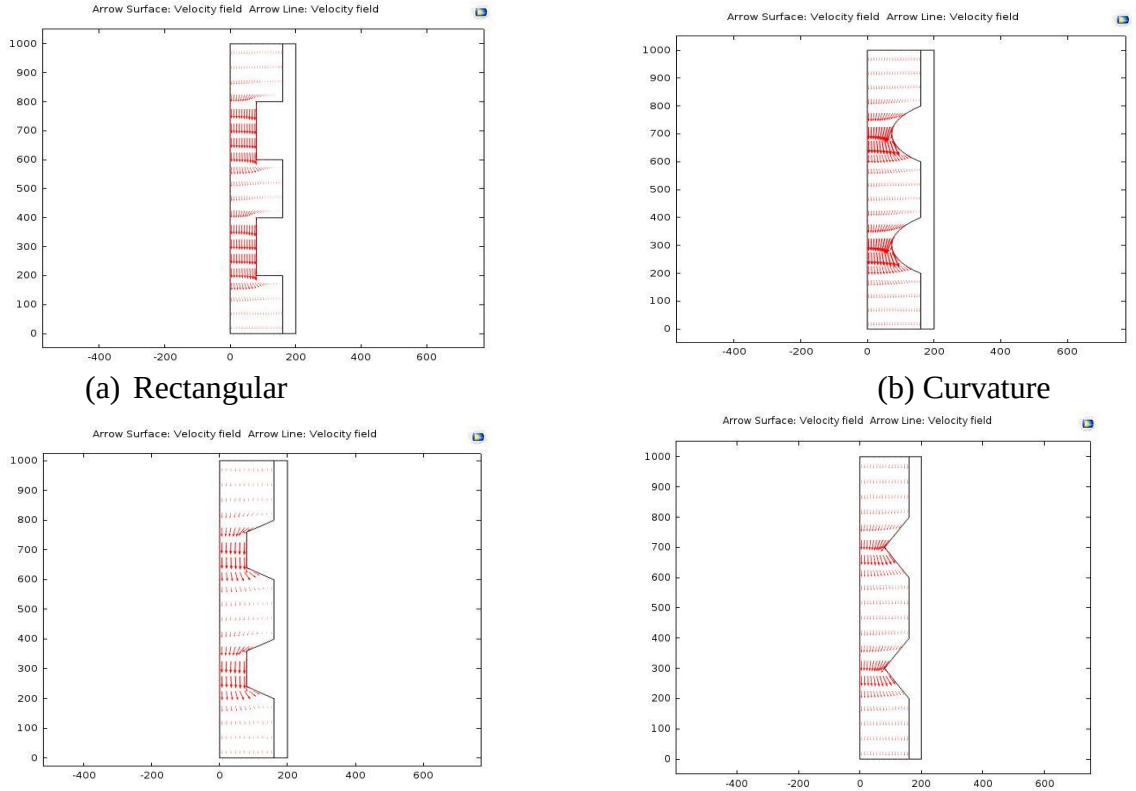

(a) Rectangular (b) Curvature

(c) Trapezoidal (d) triangular

Figure (18) Velocity stream line for microchannels with double contractions of different shapes.

Similarly, if the single contraction is replaced by a triple one, the species mixing can also be enhanced effectively. Figure 19 and Figure 20 shows the contraction profile across the channel width at the downstream position of 100µm with three contractions spaced at 80µm fixed distance. The figures demonstrate that the mixing efficiency for triple contraction microchannels has increased for triangular and rectangular contractions respectively. These incremental values are much higher their corresponding values for single contraction channels. Again, this is possibly because the flow in microchannels with triple contraction could produce multiple vortices at every contraction end. This will obviously increase the mixing efficiency by enhancing faster diffusion. Figure 20 presents a graphical evidence for this explanation.

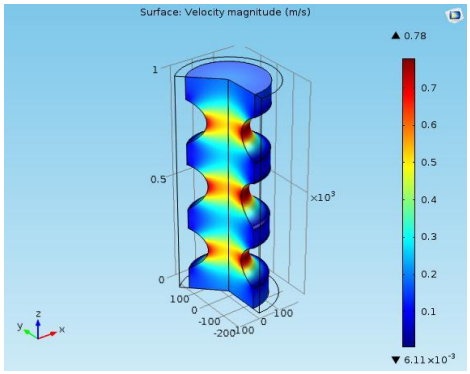

(a) Rectangular (b) Curvature

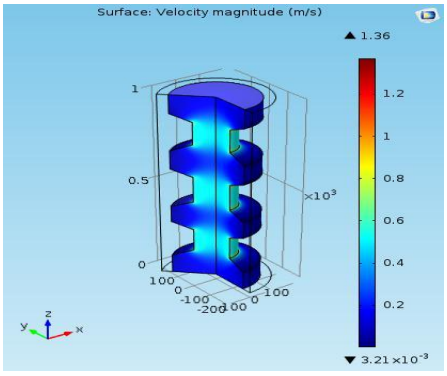

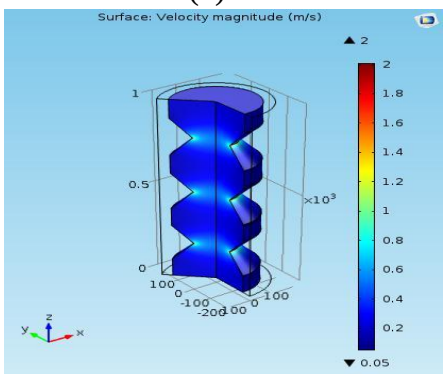

(c) Trapezoidal (d) Triangular

Figure (19) Three-dimensional contour for triple contraction microchannel with different contraction shapes.

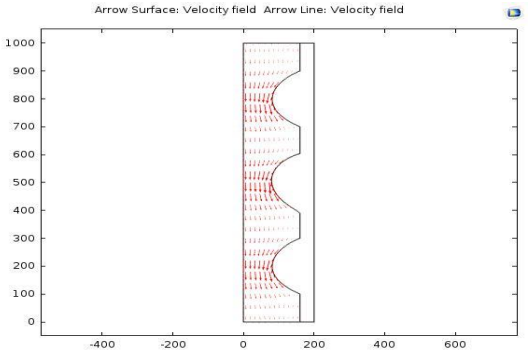

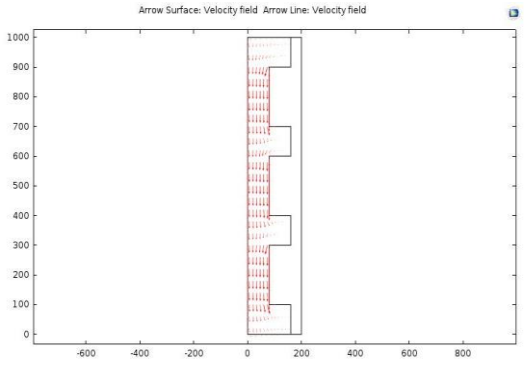

(a) Rectangular (b) Curvature

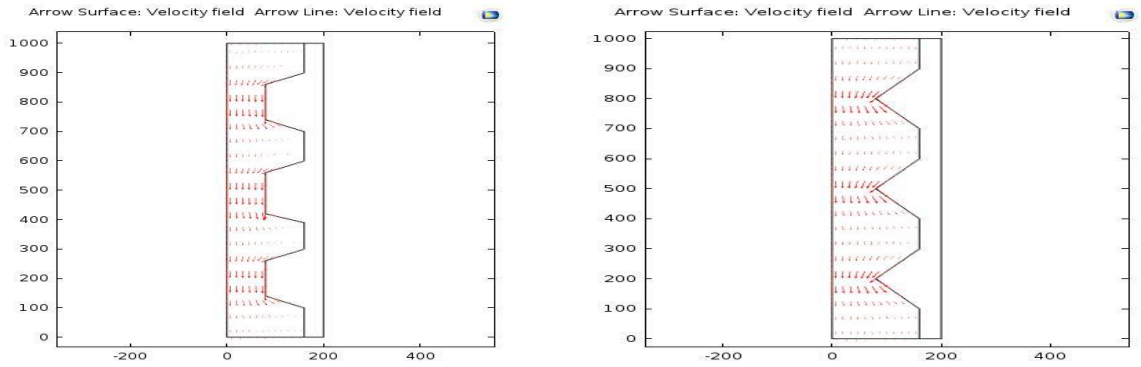

(c) Trapezoidal (d) Triangular

Figure (20) Velocity stream line for microchannels with triple contractions of different shapes.

In general, when increase number of contraction the value of electroosmosis maximum velocity will decrease.

5.conclution:

- From the contours of velocity distribution for the four shapes of contractions; rectangular, triangular, trapezoidal and curved. It is seen from these figures that the triangular contraction cause higher value for velocity.
- The temperature distribution contours for the same four microchannels with different shapes of contractions, show that, highest temperature has been recorded in the rectangular contraction case.
- In order to examine the impacts of different zeta potential values on maximum flow velocity through the four microchannels, it reveals that the maximum velocity increases as applied zeta potential increases.
- When adding materials with different thermal conductivity to channel wall can affect the heat distribution throughout channel length. In particular, five wall materials typically used in Microelectromechanical systems (MEMS). It shows that materials with low thermal conductivity work as isolation against dissipating the heat generated from Joule heating effect. In other words, low conductivity materials restrict heat transfer through channel wall and hence raising liquid temperature.

6. References:

[1] Y. Kang, C. Yang, X. Huang, Dynamic aspects of electroosmotic flow in a cylindrical microcapillary, Int. J. Eng. Sci. 40 (2002) 2203–2221.

[2] C.Y. Wang, Y.H. Liu, C.C. Chang, Analytical solution of electro-osmotic flow in a semicircular microchannel, Phys. Fluids 20 (2008) 063105.

[3] X. Xuan, D. Li, Electroosmotic flow in microchannels with arbitrary geometry and arbitrary distribution of wall charge, J. Colloid Interf. Sci. 289 (2005) 291– 303.

[4] S. Talapatra, S. Chakraborty, Double layer overlap in ac electroosmosis, Eur. J. Mech. B 27 (2008) 297–308.

[5] R.J. Yang, L.M. Fu, C.C. Hwang, Electroosmotic entry flow in a microchannel, J. Colloid Interf. Sci. 244 (2001) 173–179.

[6] D. Maynes, B.W. Webb, Fully developed electroosmotic heat transfer in microchannels, Int. J. Heat Mass Transfer 46 (2003) 1359–1369.

[7] C. Yang, D. Li, J.H. Masliyah, Modeling forced liquid convection in rectangular microchannels with electrokinetic effects, Int. J. Heat Mass Transfer 41 (1998) 4229–4249.

[8] Cheng Qi, Chiu-On Ng "Electro-osmotic Flow Through a Rotating Microchannel" Proceedings of the World Congress on Mechanical, Chemical, and Material Engineering (MCM 2015) Barcelona, Spain – July 20 - 21, 2015 Paper No. 306 .

[9] Chang‐ Yi Wang· Chun‐ Fei Kung · Chien‐ Cheng Chang " Approach to analytic solutions for electroosmotic flow in micro‐ ducts by eigenfunctions of the Helmholtz equation" Microfluid Nanofluid (2016) 20:111 DOI 10.1007/s10404-016-1764-8 page 1-13.

[10] Mushtaq I. Hasan, Alaa M. Lafta, “Study the electroosmosis flow in Microchannel with contractions of different geometries”, 2nd international scientific conference for southern technical university, Basrah, Iraq, 1-2 April, 2017.

[11]Sriram Sridharan, Joule heating effects on electrokinetic transport in contraction microchannels, M-Tech Thesis, Clemson University, May 2011.

[12] sanjay u "joule heating effects on electroosmotic flow occuring in a cylindrical contraction microchannel" Amrita school of engineering, Amritapuri campus.

[13]Electroosmotic Flow in Nanofluidic Channels Daniel G. Haywood, Zachary D. Harms, and Stephen C. Jacobson* dx.doi.org/10.1021/ac502596m | Anal. Chem. 2014, 86, 11174−11180.

[14]Electro-Osmotic Mixing in Microchannels By Pong Yu (Peter) Huang MFL TR 2002-01 Microfluidics Laboratory Division of Engineering Brown University Providence, RI 02912 September, 2002

[15]Zimmerman, W.B. and Rees, J.M. (2009) Optimal modelling and experimentation for the improved sustainability of microfluidic chemical technology design. Chemical Engineering Research and Design, 87 (6A). pp. 798-808. http://dx.doi.org/10.1016/j.cherd.2008.11.010.

[16] Mushtaq I. Hasan, Alaa M. Lafta, "Numerical investigation of electroosmotic flow in microchannel" (article in press).

[17] Mushtaq I. Hasan, Hayder M. H., Ghassan A. A., “Study of the Axial Heat Conduction in Parallel Flow Microchannel Heat Exchanger”, Journal of King Saud University – Engineering Sciences (2014) 26, 122–131.